Jupiter Publications Consortium

Vol. 1(3), pp. 125-134, 29 DEC, 2015
ISSN Print : 2454-1435 © 2015 IJRMMAE
ISSN Online : 2454-1443 © 2015 IJRMMAE
http://www.ijrmmae.in

International Journal of Research in Mechanical, Mechatronics and Automobile Engineering

Wavelet Based Image Compression System with Linear Distortion Control

Sathyanarayana M,Kumaran S, Jenitha S.
Dhanalakshmi Srinivasan College of Engineering and Technology, Chennai, India
Received 05, December 2015 | Accepted 29, December 2015

Abstract

Distortion control is an important issue in maintaining the desired quality in the retrieved signal of compressed data. A linear relationship between the distortion and quantization scale is developed, which is crucial for efficient quality maintenance and an optimized quantization of wavelet transform coefficients and low complex distortion control system for image compression is proposed in this paper. The sensitive response is caused without compromising the influences of word-length-growth (WLG) effect and unfavourable for the reconstruction quality control of ECG data compression. In this paper, the 1-D reversible round-off non-recursive discrete periodic wavelet transform is applied to overcome the WLG magnification effect in terms of the mechanisms of error propagation resistance and significant normalization of octave coefficients. This method can provide wavelet-based image data compression with a precise linear prediction model, resulting in high compression performance. The optimization can induce linear relationships among multi-level quantization scales and enable the control of multi-level quantization scales with a single variable. To produce the quantization scales formula, curve fitting technique is used which is controlled by a single value.

Keywords: Wavelet, Distortion control, Quantization scale, Linear Prediction.

1. Introduction

Now a days, through limited bandwidth channels we can transmit massive amount of real time images and this is only possible due to image compression [1]. The information area unit within the style of audio, video, graphics, and images. Through transmission process, these types of data can be compressed. During last decade, a range of wavelet based techniques have been developed for image compression [2, 3]. Encoder and decoder are based on such algorithms to minimize the number of memory [4]. Associate algorithmic rule which minimizes PSNR is delineated in [5] and it is embedded, called Rate distortion Optimized Embedding. Due to de-correlation property DWT [6] has gained so much popularity but several trendy image compression systems deals DWT as middle transform stage. When DCT was introduced, a lot of work was done on compression algorithms. Several codec algorithms were introduced to compress maximum amount of transform coefficients which amount can attainable but for this purpose we have to make a compromise between CR ratio and the quality of image. It is very difficult to achieve high compression ratio without discarding some perceptible information [5, 6, 7]. In this way it is proved that the rate of compression is application dependent. A lot of work has been done on Wavelet transforms over the last decade. For images mostly used coding algorithms based on wavelet transform are: EZW [8], STW [9], SPIHT [10] and WDR [10, 11]. For image compression, a really effective technique is wavelet coding which is considerably proved as a better algorithm than other algorithms because its efficiency is much better than other computed efficiency of image compression techniques. Now, compression systems use bi-orthogonal wavelet.

Jupiter Publications Consortium
Vol. 1(3), pp. 125-134, 29 DEC, 2015
ISSN Print : 2454-1435 © 2015 IJRMMAE
ISSN Online : 2454-1443 © 2015 IJRMMAE
http://www.ijrmmae.in
International Journal of Research in Mechanical, Mechatronics and Automobile Engineering

Bior is wavelet family it uses bi-orthogonal wavelet which is bior wavelet family. It is a real fact that it is not energy preserving but this thing can't effect its use because it is not a huge drawback. Now we are going to differentiate between orthogonal wavelet and bi-orthogonal wavelet. The main difference is that in orthogonal wavelet associated wavelet transform is orthogonal but in bi-orthogonal wavelet, the associated wavelet transform is invertible however not essentially orthogonal but there are some coefficients of linear phase bi-orthogonal filter which are so much close to bi-orthogonal. Bi-orthogonal wavelet has symmetric filters and it also permits the employment of a way broader category of filters. Linear phase filters are used in bi-orthogonal wavelet transform so this is so much advantageous in this sense because with the help of symmetric inputs we can obtain symmetric outputs which are given once. With the help of this transform we can solve many issues like coefficient expansion [12] and broader discontinuities.

A.

2. Nonlinear Quantization Scheme with Linear Distortion Characteristic

Essentially, the goal of the iterative process of error control loop is to refine the quantization scales of all decomposition levels until the distortion is located in a tolerable region. The refining process needs to predict a quantization scale for next iteration. Linear prediction model can be one of the favourites due to its simplicity and efficiency. However, linear prediction model can only be suitable for linear compression performance. In this section, a new multivariable quantization scheme based on the 1-D RRO-NRDPWT and the significance normalization process is developed. The quantization scale design is conducted according to three criteria: 1) using a variable QF to determine the quantization scales of all decomposition levels; 2) maintaining the three variables: PRD, CR, and QF, in linear relationship; and 3) decreasing the gradient of the PRD–CR curve.

Let d^*_j be a vector encompassing reversible wavelet coefficients of the j^{th} level. The quantization process can be defined as follows:

$$S^*_0=tr(s^*_0/b_{DC}) \text{ and } d^*_j=tr(d^*_j/c_j) \quad (1)$$

where tr(d∗j) denotes the truncation process that truncates each element of d^*_j to an integer, and b_{DC} and C_j are quantization scales of the j^{th} level. In the inverse quantization process, each retrieved datum will be compensated by half of the quantization scale, namely

$$S^*_0 \text{ and } d^*_j=b_{DC}(s^*_0+0.5sign(s^*_0))=c_j\ (d^*_j+0.5sign(d^*_j)) \quad (2)$$

where sign(d^*_j) denotes the sign vector of d^*_j, e.g., given d^*_j =[−2,3]; then sign (d^*_j)=[−1,1]. For the determination of quantization scales, we define c_j as follows:

$$C_j=C_p[j]\ SNFj \quad (3)$$

where SNFj is the significance normalization factor and $C_p[j]$ is an adjustable parameter.

By using a dataset (given in Section V), the influence of $C_p[j]$ is explored in Figs. 1 and 2, where the mean values of entropy and PRD of each level are depicted, respectively. In comparison with the round-off process [15], the curves derived by the two methods are similar in shape, except for the scale. This similarity is a result of the significance normalization of octave coefficients. With the same PRD value, the truncation process can yield less entropy. This implies that the compression performance of the truncation process can also be improved. The significance normalization mechanism can effectively reduce the searching area of $C_p[j]$ in an 11-dimensional space to obtain an

Jupiter Publications Consortium
Vol. 1(3), pp. 125-134, 29 DEC, 2015
ISSN Print : 2454-1435 © 2015 IJRMMAE
ISSN Online : 2454-1443 © 2015 IJRMMAE
http://www.ijrmmae.in
International Journal of Research in Mechanical, Mechatronics and Automobile Engineering

approximately linear PRD–CR curve. Based on the similarity, we choose 16 points in the PRD–CR curve derived in [15]. For each point, the corresponding $C_p[j]$ for j=0,−1,…,−9 was multiplied by a scalar, with the new scale $C_p[j]$ used as the centroid of a searching area. By using (3) and (4), the selection of new quantization scales $C_p[j]$ from 16 areas is based on a line fitting method that minimizes both the gradient and least square error. Here, we note that the new $C_p[j]$ is by no means a globally optimal solution due to the restriction of searching area. Finally, we define a polynomial function $f_j(x)$ for each octave to fit the $C_p[j]$ values with 16 integers, namely, fj(QF)=cp[j] for QF=1,…,15.

The $C_p[j]$ determined by some values of QF is shown in Fig. 3. In Fig. 3, it is observable that three high octaves $C_p[j]$; $j = 0, -1, -2$, are maintained in small values even in a high CR situation. For the low octaves $-9 \le j \le -4$, the cp[j] curve is approximately linear for each QF and the gradient of the curve increases very fast with respect to QF. As shown in Fig. 6, each QF can provide a set of nonlinear quantization scales for all levels.

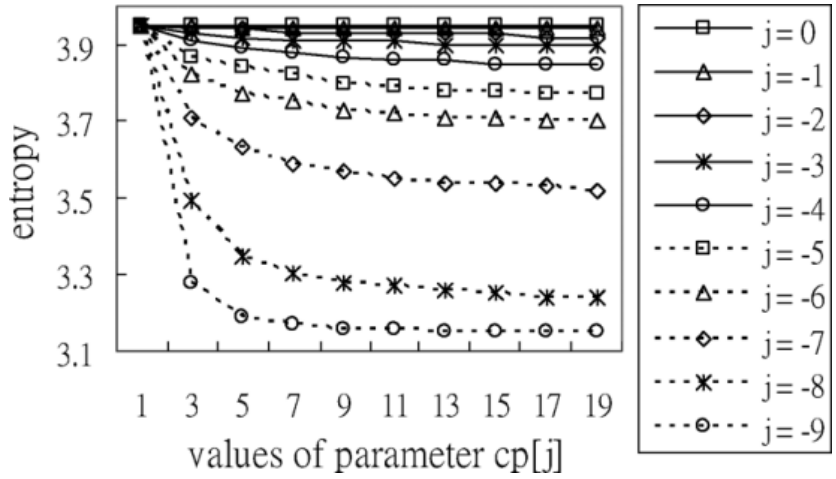

Fig 1. Influence on entropy by $C_p[j]$.

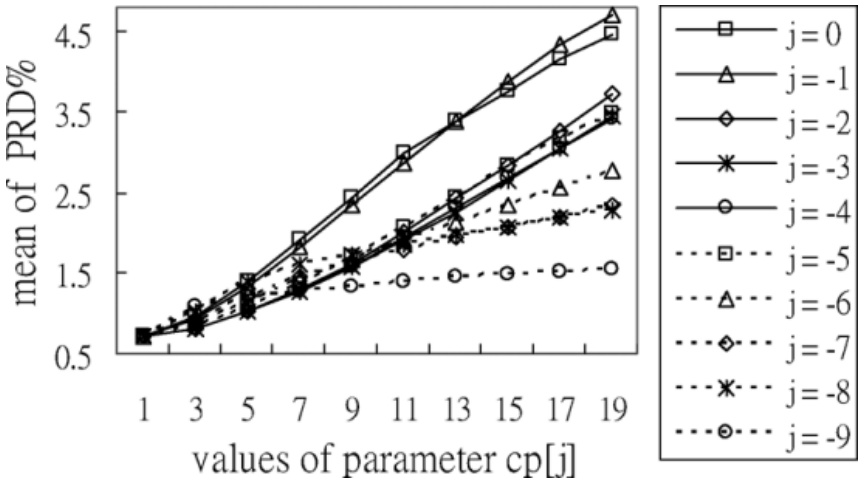

Fig 2. Influence on PRD by $C_p[j]$.

Jupiter Publications Consortium
Vol. 1(3), pp. 125-134, 29 DEC, 2015
ISSN Print : 2454-1435 © 2015 IJRMMAE
ISSN Online : 2454-1443 © 2015 IJRMMAE
http://www.ijrmmae.in
International Journal of Research in Mechanical, Mechatronics and Automobile Engineering

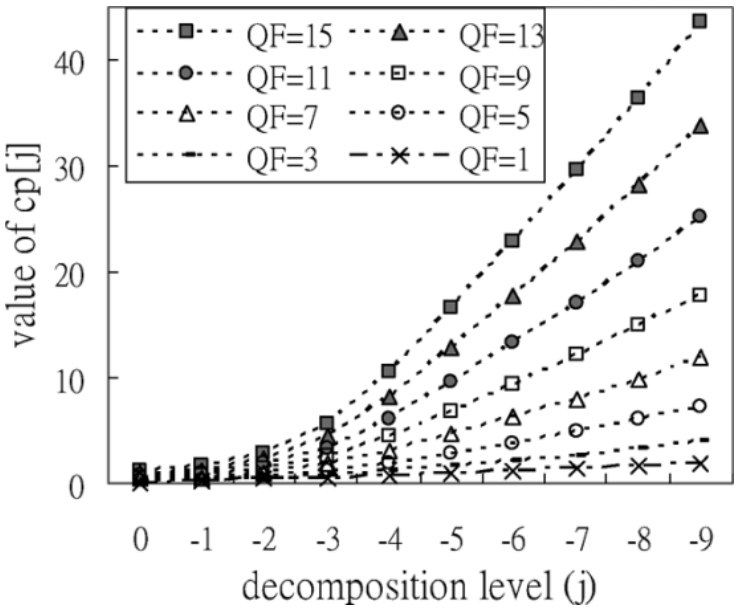

Fig 3. Values of $C_p[j]$ determined by the factor QF. Note that QF=2n lies between QF=2n−1 and QF=2n+1.

For exploring the linear control performance of QF, all 48 ECG signals recorded in the MIT-BIH arrhythmia database were used. Each signal contains about a 15-min length of sampled data. The investigation results are depicted in Fig. 4, where large variance can be found for QF>16. However, Fig. 4 reveals that an approximately linear relationship between PRD and QF can be obtained for all signals with different gradients.

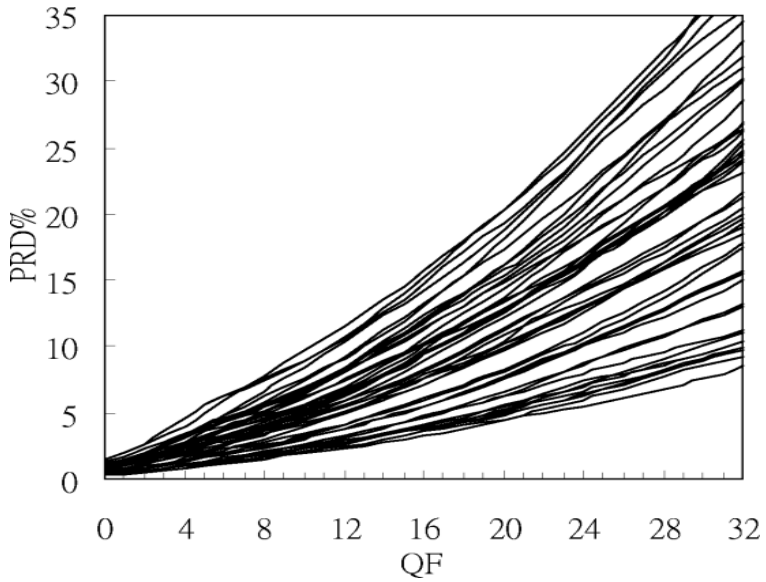

Fig 4. PRD–QF curves of 48 ECG signals derived by the proposed quantization scheme.

B.
C.
D.

3. *Linear Prediction Algorithm for High Efficient Error Control Loop*

Jupiter Publications Consortium
Vol. 1(3), pp. 125-134, 29 DEC, 2015
ISSN Print : 2454-1435 © 2015 IJRMMAE
ISSN Online : 2454-1443 © 2015 IJRMMAE
http://www.ijrmmae.in
International Journal of Research in Mechanical, Mechatronics and Automobile Engineering

An RRO-NRDPWT-based ECG data compression system with linear quality control function is shown in Fig. 5, where the dashed-line block indicates the functional processes of an error control loop. PRDT, denoting the target PRD, is a specified value. The error control loop requires two buffers for temporarily saving a segment of originally sampled data SJ and reversible transformed data d*, respectively. At the beginning of each segment, coefficients d* will be fed into the error control loop and a buffer. The data temporarily saved in the buffer are used for an iterative quantization process. Quantized data đ* can be further compressed by lossless SPIHT encoder only when the distortion is less than a tolerable bound. This design can effectively reduce the power consumption of SPIHT encoding and data transmission.

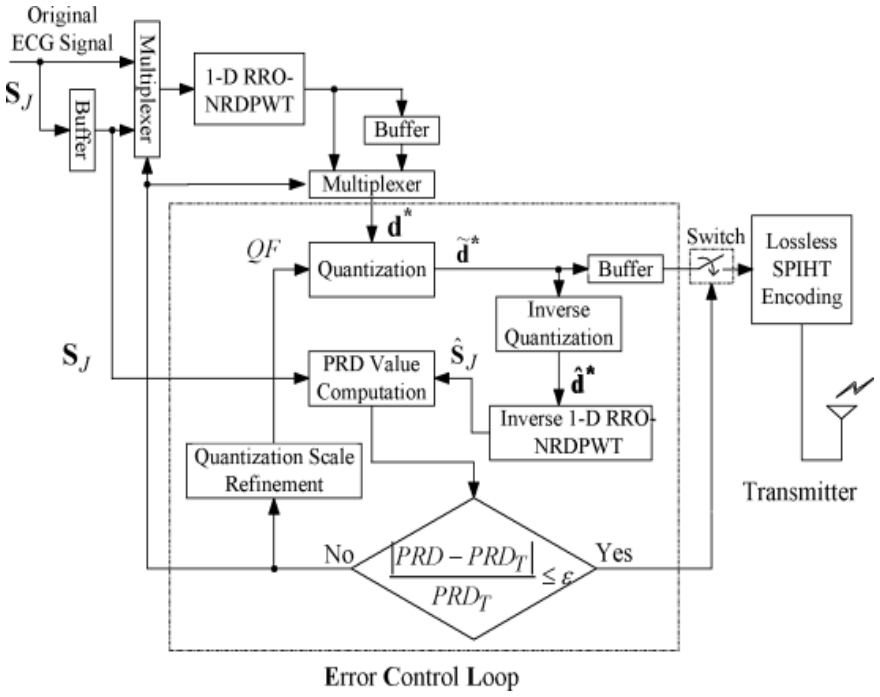

Fig 5. RRO-NRDPWT-based ECG data compression system with reconstruction quality guaranteed function.

The error control loop procedure is described as follows.

PRD_T a target for retrieved quality of quantized coefficients, ε tolerable bound defined in Fig. 5.

1. Set the parameters and let loop=0, $QF_0=QF_{default}$.
2. Refine quantization scale with a linear QF prediction algorithm defined as follows:

1. If loop=1, set

a) $$QF_{loop} = aQ_{Floop-1}+(a-1)\Delta$$

b) $$\text{where } a = PRD_T/PRD_{loop-1}.$$

2. If loop>1, set

c) $$QF_{loop}=QF_{loop-1}+b(QF_{loop-1}-QF_{loop-2})$$

d) $$\text{where } b=(PRD_T-PRD_{loop}-1/PRD_{loop-1}-PRD_{loop-2}).$$

3. Quantize wavelet coefficients d* using: QF_{loop}.
4. Take inverse quantization and inverse 1-D RRO-NRDPWT.

5. Compute the value of PRD

Jupiter Publications Consortium
Vol. 1(3), pp. 125-134, 29 DEC, 2015
ISSN Print : 2454-1435 © 2015 IJRMMAE
ISSN Online : 2454-1443 © 2015 IJRMMAE
http://www.ijrmmae.in
International Journal of Research in Mechanical, Mechatronics and Automobile Engineering

6. Control the quality with a logic decision given in the following:

   If($|PRD-PRD_T|)/PRD_T>\varepsilon$, then loop=loop+1; select data from buffer; go to Step 2;
   else

   $QF_0=QF_{loop}$ assign the initial QF for the next segment; loop=0; close the switch for saving compressed data; go to Step 2.

QF is a quality control parameter used to determine the quantization scale. For reconstruction, QF value should be transmitted before the transmission of compressed ECG data. With this aim, it is desirable to represent QF value with an integer. The linearity of PRD–QF curve permits QF value representation using uniform quantization without the cost of precision and convergence speed in a low bit rate situation. After investigating all the ECG signals in the MIT-BIH arrhythmia database, it is sufficient to range QF value from 0 to 32. This range will be uniformly quantized into 512 levels with quantization steps equal to 0.0625. In Step 2, the computed QF_{loop} value will be assigned to the nearest quantization level. $QF_{default}$ denotes a default QF value used for the first segment of a signal when loop=0. A proper $QF_{default}$ is useful for increasing the convergence speed of the first segment; for this sake, we use the average PRD–QF curve derived from Fig. 4 for $QF_{default}$ determination with

$$QF_{default}=PRD_T3221.96-0.76+0.76. \quad (4)$$

Similarly, the value derived in (4) will be assigned to the nearest quantization level. The three $QF_{default}$ are 5.3125, 9.8125, and 14.375, corresponding to PRDT= 3%, 6%, and 9%, respectively. Here, we note that the $QF_{default}$ values can be only suitable for the MIT-BIH arrhythmia database. For other segments, the QF0 of current segment is assigned as the final QF (i.e., QF_{loop}) of the previous segment. The experiments using all of the ECG signals in the MIT-BIH arrhythmia database show that with this initial QF definition, 20% of all of the segments can achieve convergence in the first loop without the need for iteration.

4. Experimental Results and Discussion

For system realization, it is desirable to reduce the computational complexity and iterations of the error control loop. Theoretically, the convergence can be achieved within two iterations when the relationship between PRD and QF is exactly linear, because the compensation Δ defined in the linear QF prediction model is a constant for each signal. However, the experiments showed that iterations increased as PRD_T was increased. This implies that the actual PRD–QF curve is not linear due to the use of fixed quantization scales. Generally, a more linear PRD–QF curve can obtain faster convergence speed and more precise control. Without losing the generality, the same reconstruction quality control scheme associated with the same quantization scale is also applied for the 28 signals in the MIT-BIH ST change database [29].

Lossy ECG data compression is meaningful only when the clinical information can be preserved. The study in [23] claimed that the energy spectrum of QRS complex will range from 1 to 40 Hz, and almost centered around 17 Hz. The T-wave recording the action of ventricular repolarisation always appears after the QRS complex and can occur in various shapes. The frequency distribution of T-wave is almost below 6 Hz. The duration of the P-wave recording the action of atrial depolarization generally is about 100 ms. The P-wave normally appears before the QRS complex, but some heart diseases may cause the P-wave to appear at different locations with every beat. The frequency distribution of the P-wave is

Jupiter Publications Consortium
Vol. 1(3), pp. 125-134, 29 DEC, 2015
ISSN Print : 2454-1435 © 2015 IJRMMAE
ISSN Online : 2454-1443 © 2015 IJRMMAE
http://www.ijrmmae.in
International Journal of Research in Mechanical, Mechatronics and Automobile Engineering

almost below 10 Hz [24]. These studies claimed that the clinical information, including the ST segment [29], only occupies a low-frequency spectrum. For a sampling rate of 360 Hz, clinical information will be dominantly involved in the wavelet coefficients d^*_j with $j \geq -7$, where the bandwidths of levels $j=-7$ and -6 are 8.4–45.7 Hz and 4.2–22.5 Hz, respectively. A detailed frequency bandwidth description of wavelet channel filters can be found in [29]. The relative quantization error analysis between levels is helpful for comprehending the capability of clinical information preservation in the quantization scheme. For this purpose, an experiment of quantization process for QF=1, 2,…,23 was taken. The transformed data were simulated with random numbers generated in the range of [500, −500], where 100 random datasets were used. For each QF, the quantization errors of each octave (i.e., $j=-9$ to 0) were calculated and inversely transformed for computing the reconstruction error $Ej=(|err_{ji}|)/N$, where err_{ji} denote the reconstructed error provided by the j^{th} octave's quantization errors. The percentage of the relative reconstruction errors defined as $(\sum_{100}E_j/\sum_{100}E_{-7})*100\%$ is shown in Fig. 6. For QF=1, the percentage value becomes large because the reconstruction error of $j=-7$is very small. In general, the reconstruction error will be fast decreased as the level is increased. This property can effectively diminish clinical information loss in high CR situation. An ECG data compression result is demonstrated in Fig. 7. In Fig. 7(b), a reconstruction of low CR case, the reconstructed signal is smoother than the original signal, but shape can be kept well. A result of high CR case is shown in Fig. 7(c) and (d), which is derived with RRO-NRDPWT and SPIHT schemes, respectively. The two examples show that notable shape distortion will first appear around the QRS complex (before and after) when CR is increased.

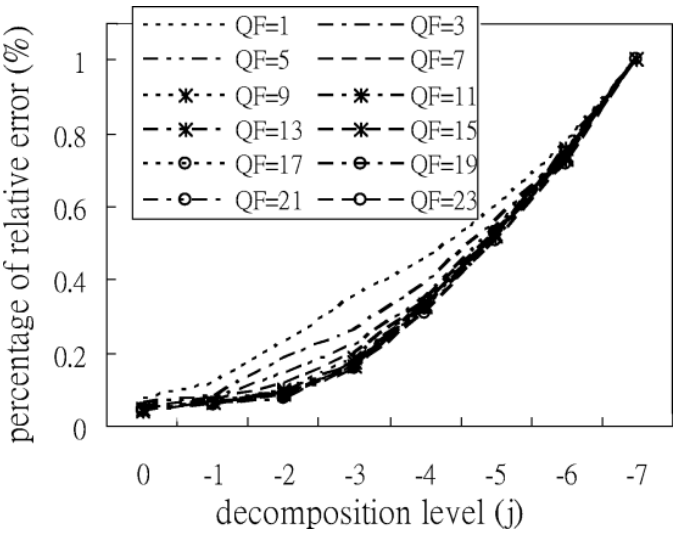

Fig 6. Relative reconstruction error induced by the quantization scale of every level.

Jupiter Publications Consortium
Vol. 1(3), pp. 125-134, 29 DEC, 2015
ISSN Print : 2454-1435 © 2015 IJRMMAE
ISSN Online : 2454-1443 © 2015 IJRMMAE
http://www.ijrmmae.in
International Journal of Research in Mechanical, Mechatronics and Automobile Engineering

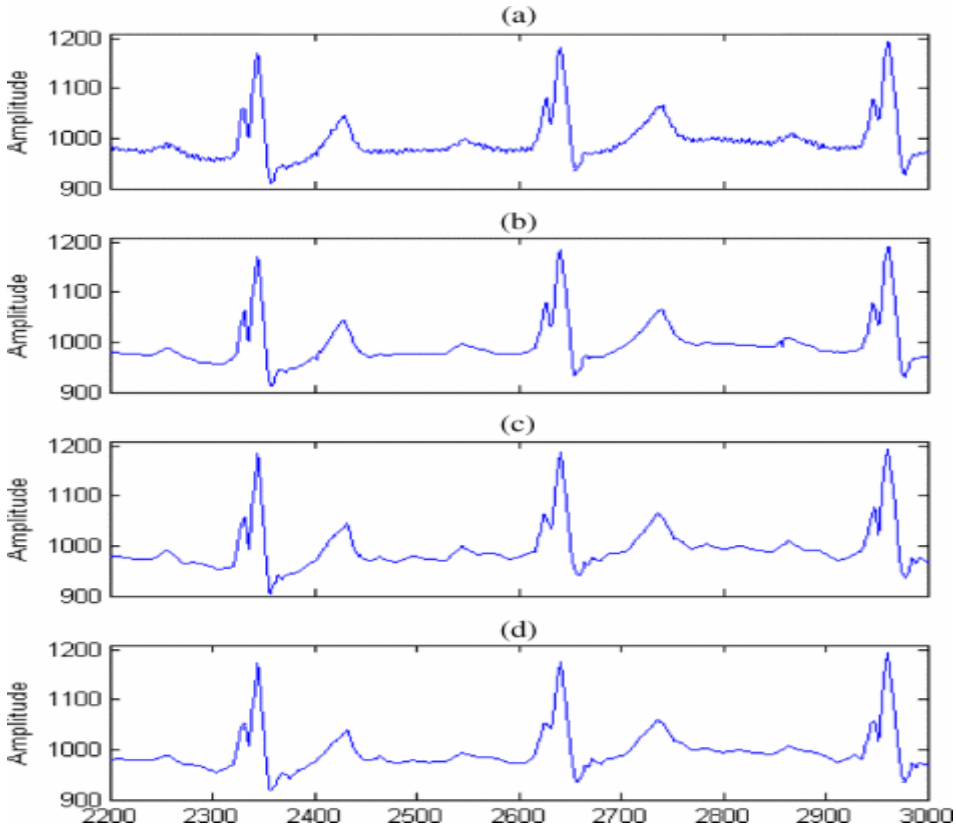

Fig 7. Demonstration of some ECG data compression results. (a) Original signal. (b) Reconstruction of low CR case. (c) and (d) Reconstruction of high CR case in using two compression methods.

The computational complexities required for variant wavelet-based quality control methods are shown in Table IX. Using an IBM PC with MS Windows XP, Pentium-4 3.4GHz CPU, and 512 MB RAM, the execution time (T) of an error control loop of the proposed system was found as $T=t(\text{quantization})+t(\text{quantization}^{-1})+t(\text{RRO}-\text{NRPDWT}^{-1})+t(\text{PRD})=0.095+0.057+0.252+0.083=0.487$ms. This implies that for loop≥3, the process of error control loop cannot be finished during a sampling period. Based on the results here, it is concluded that with high-quality control, the proposed system can satisfy the real-time requirement in most cases.

E.

5. *Conclusion*

F.

The quantization design is based on the 1-D RRO-NRDPWT that can effectively eliminate the WLG magnification effect and facilitates significant normalization of octave coefficients. For reconstruction quality control, an efficient multivariable quantization scheme with linear distortion characteristic has been developed in this paper. The quantization scheme has robust capability for preserving clinical information in high CR situation. With the advantages of single control variable and linear compression performance, a linear quantization scale prediction model is also presented for efficient reconstruction quality control. Experimental results based on the MIT-BIH arrhythmia database reveal that the proposed system is superior to other wavelet-based approaches in regard to both compression and reconstruction quality control performances.

Vol. 1(3), pp. 125-134, 29 DEC, 2015
ISSN Print : 2454-1435 © 2015 IJRMMAE
ISSN Online : 2454-1443 © 2015 IJRMMAE
http://www.ijrmmae.in
International Journal of Research in Mechanical, Mechatronics and Automobile Engineering

6. References

1. DeVore R.A., Jawerth B., Lucier B.J., "Image Compression Through Wavelet Transform Coding". *IEEE Transactions on Information Theory*, 38, 2, 719−746, March 1992.
2. Islam A., Pearlman W.A., "An Embedded and Efficient Low-Complexity Hierarchical Image Coder". *In Proc. of SPIE 1999, Visual Communications and Image Processing*, San Jose, CA, 3653, 294−305, Jan. 1999.
3. Jai A., Potnis A., "Wavelet Based Video Compression Using STW, 3D-SPIHT & ASWDR Techniques: A Comparative Study", *International Journal of Advances in Engineering & Technology*, 3, 2, 224−234, 2012.
4. Kim B.J., Pearlman W.A., "An Embedded Wavelet Video Coder Using Three Dimensional Set Partitioning in Hierarchical Trees (3D-SPIHT)" *In Proc. of Data Compression Conference 1997*, Snowbird, USA, 251−260, March 1997.
5. Kim B.J., Xiong Z., Pearlman W.A., "Low Bit-Rate Scalable Video Coding with 3-D Set Partitioning in Hierarchical Trees (3-D SPIHT)", *IEEE Transactions on Circuits and Systems for Video Technology*, 10, 1374−1387, Dec. 2000.
6. Lewis A.S., Knowles G., "Image Compression Using the 2-D Wavelet Transform" *IEEE Transactions on Image Processing*, 1, 2, 244−250, April 1992.
7. Li J., Lei S., "An Embedded Still Image Coder with Rate-Distortion Optimization", *IEEE Transactions on Image Processing*, 8, 7, 913−924, 1999.
8. Malvar H., "Progressive Wavelet Coding of Images", *In Proc. of IEEE Data Compression Conference* (DCC'99), Salt Lake City, UT, 336−343, March 1999.
9. Namuduri K.R., Ramaswamy V.N., "Feature Preserving Image Compression", *Pattern Recognition Letters*, 24, 15, 2767−2776, Nov. 2003.
10. Negahdaripour S., Khamene A., "Motion-based Compression Of underwater Video Imagery for Operations of Unmanned Submersible vehicles" *Computer Vision and Image Understanding*, 79, 1, 162−183, 2000.
11. R. Nygaard, G. Melnikov, A. K. Katsaggelos, "A rate distortion optimal ECG coding algorithm", *IEEE Trans. Biomed. Eng.*, vol. 48, no. 1, pp. 28-40, Jan. 2001.
12. Y. Zigel, A. Cohen, A. Katz, "ECG signal compression using analysis by synthesis coding", *IEEE Trans. Biomed. Eng.*, vol. 47, no. 10, pp. 1308-1316, Oct. 2000.
13. R. Benzid, F. Marir, A. Boussaad, M. Benyoucef, D. Arar, "Fixed percentage of wavelet coefficients to be zeroed for ECG compression", *Electron. Lett.*, vol. 39, no. 11, pp. 830-831, May 2003.
14. Z. Lu, D. Y. Kim, W. A. Pearlman, "Wavelet compression of ECG signals by the set partitioning in hierarchical trees (SPIHT) algorithm", *IEEE Trans. Biomed. Eng.*, vol. 47, no. 7, pp. 849-856, Jul. 2000.
15. C. T. Ku, H. S. Wang, K. C. Hung, Y. S. Hung, "A novel ECG data compression method based on nonrecursive discrete periodized wavelet transform", *IEEE Trans. Biomed. Eng.*, vol. 53, no. 12, pp. 2577-2583, Dec. 2006.
16. Alesanco, J. Garcia, P. Serrano, L. Ramos, R. S. H. Istepanian, "On the guarantee of reconstruction quality in ECG wavelet codecs", *Proc. 28th IEEE EMBS Annu. Int. Conf.*, pp. 6461-6464, 2006-Aug.
17. T. Blanchett, G. C. Kember, G. A. Fenton, "KLT-based quality controlled compression of single-lead ECG", *IEEE Trans. Biomed. Eng.*, vol. 45, no. 7, pp. 942-945, Jul. 1998.

Vol. 1(3), pp. 125-134, 29 DEC, 2015
ISSN Print : 2454-1435 © 2015 IJRMMAE
ISSN Online : 2454-1443 © 2015 IJRMMAE
http://www.ijrmmae.in
International Journal of Research in Mechanical, Mechatronics and Automobile Engineering

18. M. Blanco-Velasco, F. Cruz-Roldan, J. I. Godino-Llorente, K.E. Barner, "ECG compression with retrieved quality guaranteed", *Electron. Lett.*, vol. 40, no. 23, pp. 1466-1467, Nov. 2004.
19. R. Benzid, F. Marir, N.-E. Bouguechal, "Electrocardiogram compression method based on the adaptive wavelet coefficients quantization combined to a modified two-role encoder", *IEEE Signal Process. Lett.*, vol. 14, no. 6, pp. 373-376, Jun. 2007.
20. J. Chen, S. Itoh, "A wavelet transform-based ECG compression method guaranteeing desired signal quality", *IEEE Trans. Biomed. Eng.*, vol. 45, no. 12, pp. 1414-1419, Dec. 1998.
21. S. G. Miaou, C. L. Lin, "A quality-on-demand algorithm for wavelet-based compression of electrocardiogram signals", *IEEE Trans. Biomed. Eng.*, vol. 49, no. 3, pp. 233-239, Mar. 2002.
22. C.-T. Ku, "A high efficient ECG data compression system based on reversible round-off discrete wavelet transform", *Doctoral Dissertation Inst. Eng. Sci. Technol. Nat. Kaohsiung First Univ. Sci. Technol.*, 2007-May.
23. Y. Zigel, A. Cohen, A. Katz, "The weighted diagnostic distortion (WDD) measure for ECG signal compression", *IEEE Trans. Biomed. Eng.*, vol. 47, no. 11, pp. 1422-1430, Nov. 2000.
24. S. Al-Fahoum, "Quality assessment of ECG compression techniques using a wavelet-based diagnostic measure", *IEEE Trans. Inf. Technol. Biomed.*, vol. 10, no. 1, pp. 182-191, Jan. 2006.
25. F. Tsai, H. S. Wang, K. C. Hung, "A high efficient nonrecursive discrete periodized wavelet transform for extracting the transformed coefficients of coarser resolution levels", *Proc. 2004 IEEE Asia-Pacific Conf. Circuits Syst.*, pp. 661-664, Dec. 69.
26. G. B. Moody, R. G. Mark, "The impact of the MIT/BIH arrhythmia database", *IEEE Eng. Med. Biol. Mag.*, vol. 20, no. 3, pp. 45-50, May/Jun. 2001.
27. K. C. Hung, "The generalized uniqueness wavelet descriptor for planar closed curves", *IEEE Trans. Image Process.*, vol. 9, no. 5, pp. 834-845, May 2000.
28. K. C. Hung, Y. S. Hung, Y. J. Huang, "A nonseparable VLSI architecture for 2-D discrete periodized wavelet transform", *IEEE Trans. VLSI Syst.*, vol. 9, no. 5, pp. 565-576, Oct. 2001.
29. O. T. Inan, L. Giovangrandi, G. T. A. Kovacs, "Robust neural-network-based classification of premature ventricular contractions using wavelet transform and timing interval features", *IEEE Trans. Inf. Technol. Biomed.*, vol. 53, no. 12, pp. 2507-2515, Dec. 2006.